Progress of Theoretical Physics, Vol. 67, No. 5, May 1982

Coupled-Discretized-Continuum-Channels Method for Deuteron Breakup Reactions Based on Three-Body Model

—— *Justification of the Method for Truncation and Discretization of the p-n Continuum* ——

Masanobu YAHIRO,[†] Masahiro NAKANO,* Yasunori ISERI and Masayasu KAMIMURA

Department of Physics, Kyushu University, Fukuoka 812
**Division of Physics, University of Occupational and Environmental Health, Kitakyushu 807*

(Received November 13, 1981)

For the treatment of the deuteron breakup process, the p-n continuum states are truncated for linear and angular momenta as $k \leq k_{max}$ and $l \leq l_{max}$, respectively, and a finite number of p-n breakup channels are introduced by discretizing the p-n continuum into momentum bins with a common width Δk. Validity and usefulness of this method are shown through crucial examinations on the $d+^{58}$Ni system at the deuteron incident energy of 80 MeV. The S-matrix elements converge smoothly and rapidly with respect to narrowing Δk in the cases both of the exact Hamiltonian and the adiabatic Hamiltonian. In the latter case, it is explicitly shown that the converged S-matrix elements agree with the exact ones. Sufficient convergence of the breakup S-matrix elements is seen at $\Delta k = 1/8$ fm^{-1} and that of the elastic ones at $\Delta k = 1/4$ fm^{-1}. The S-matrix elements also converge quickly with respect to increasing k_{max} and l_{max}. Physically sufficient truncation is given by $k_{max} \sim 1.0$ fm^{-1} and $l_{max} = 2$.

§ 1. Introduction

In deuteron induced reactions, the deuteron breakup is an important process which gives significant effects on the elastic and other reaction channels.[1)~8)] In order to study the mechanism of deuteron induced reactions, one has to solve the scattering problem of at least three bodies. Such a three-body model has been the basis of most previous theoretical analyses of deuteron induced reactions and is also the basis of the present work.

With the use of separable potentials, N-d scattering[9)] and d-^{4}He scattering[10)] have extensively been studied on the basis of the Faddeev theory[11)] for the three-body problem. Methods with the use of local potentials in the framework of the theory were proposed and so far applied to low-energy N-d scattering[12)] and bound states of three nucleon systems.[13)] The theory, however, has not been applied to heavier systems with Coulomb potentials or absorptive imaginary potentials.

A straightforward coupled-channels (CC) approach for the three-body system

[†] Present address: Shimonoseki University of Fisheries, Shimonoseki 759-65.

with full continuous states of the p-n system has well-known difficulties.[14] The CC equations, however, become soluble in the truncated model space with a limitation of linear and angular momenta of the p-n system, k and l respectively, because the kernel of the integral form of the CC equations is compact within the model space.[15] The present CC approach with the upper limit $k_{\max}$ and $l_{\max}$ is based upon the above theoretical consideration. In actual CC calculations, it is inevitable to use a finite number of the p-n relative wave functions obtained by discretizing the p-n continuum spectrum. Hereafter, we refer to the CC method with the use of such discretized p-n wave functions as the coupled-discretized-continuum-channels (CDCC) method. Two types of such methods have so for been utilized.

CDCC method I: The continuum spectrum of the p-n internal Hamiltonian, H_{pn}, is discretized into momentum bins. The discrete p-n wave functions are made by averaging the eigenfunctions of H_{pn} in each momentum bin.[2),3),8)]

CDCC method II: The discrete p-n wave functions are given by the diagonalization of H_{pn} in the subspace spanned by a finite number of basis functions which are damping asymptotically.[4),5),7)]

In the method II, the total wave function does not have breakup components in the asymptotic region and the breakup S-matrix elements cannot be obtained from its asymptotic amplitudes. Furthermore, it is difficult to adjust the basis functions so as to obtain a desired level density distribution. As seen in Ref. 5), it is not simple to obtain a sufficiently uniform high level density, because an addition of basis functions may contribute mainly to increasing the upper boundary of the p-n energy spectrum and/or to increasing the level-density near p-n zero energy. As a consequence of this property, the method II is not suitable for analyzing the role of each energy (momentum) region of the p-n continuum.

In contrast, the method I is suited for calculating the breakup S-matrix elements on account of the correct asymptotic behaviour of the p-n wave functions. Furthermore, we can easily set up the p-n discrete wave functions with any desired level density by simply narrowing the width of the momentum bins, Δk; the p-n continuum can be obtained in the limit $\Delta k \to 0$. It is, therefore, interesting to investigate the convergence of the S-matrix elements and cross sections with respect to narrowing Δk in order to examine the validity of the CC approach based on the method I.

Such an examination of the CDCC method was first done on the $d+{}^4\mathrm{He}$ system.[8b)] Clear convergence of the elastic and breakup S-matrix elements was exhibited for narrowing Δk and increasing $k_{\max}$. The investigation, however, was limited to the case $l=0$. Since the importance of the $l=2$ (d-wave) breakup states has been pointed out,[2),6)] it is necessary to carry out the same study including the s- and d-waves.

Since the present investigations are all performed on the CDCC method I,

hereafter we call it simply the CDCC method.

The purposes of the present paper are the following. One is to investigate the validity of the CDCC method by examining the convergence of the CDCC solution with respect to narrowing Δk including s- and d-waves. The examination is performed for the exact three-body Hamiltonian and for the adiabatic three-body Hamiltonian. In the latter case, the results are compared with the exact solution obtained by the method of Amakawa et al.[6] The other purpose is to examine $l_{\max}$ and $k_{\max}$ which give a physically sufficient truncation of the model space for the CDCC calculation by checking the convergence of the S-matrix elements with respect to increasing $l_{\max}$ and $k_{\max}$. We perform these examinations on the $d+^{58}$Ni system at the deuteron incident energy, $E_d=80$ MeV. We show the validity and the usefulness of the CDCC method and present adequate values of $l_{\max}$, $k_{\max}$ and Δk.

The rearrangement channels are neglected in the present paper. It was shown, however, in Ref. 5) that the effect of the coupling of the proton channel upon the deuteron and deuteron distortion channels is rather small except at lower incident energies ($E_d \lesssim 20$ MeV) in the case of $p+^{17}$O$(2s)$ channel coupling in $d+^{16}$O system. It seems that except at lower energies, the cross sections for the rearrangement channels can be calculated by the Born approximation.

In the present work, the antisymmetrization between deuteron and target nucleons is not considered. In the light of Ref. 8), however, it is likely that the antisymmetrization does not significantly affect the present examinations.

In § 2, we reformulate the CDCC method of Refs. 2) and 8). In § 3, we examine convergence of its solution with narrowing Δk. In § 4, the convergence with increasing $l_{\max}$ and $k_{\max}$ is shown. The conclusions are given in § 5.

§ 2. Formulation

2.1. *Coupled-continuum-channels method*

Neglecting total antisymmetrization and target excitation, we introduce the Hamiltonian of the $p+n+A$ system as

$$H=-\frac{\hbar^2}{2\mu_R}\nabla_R^2+U_{nA}(r_{nA})+U_{pA}(r_{pA})+U^{(\mathrm{Coul})}(R)+H_{pn}\,, \tag{2·1}$$

$$H_{pn}=-\frac{\hbar^2}{2\mu_\rho}\nabla_\rho^2+V_{pn}(\rho). \tag{2·2}$$

The p-n c.m. coordinate with respect to the core nucleus is denoted by $\boldsymbol{R}$ and the p-n relative coordinate by $\boldsymbol{\rho}$. The p-n potential is V_{pn} and U_{nA}, U_{pA} are nuclear parts of the nucleon-core potentials. The Coulomb potential, $U^{(\mathrm{Coul})}$, is evaluated

at the centre of mass of the deuteron.*) Non-central components of U_{nA}, U_{pA} and V_{pn} are neglected for simplicity and we neglect the spin wave functions.

The total wave function, Ψ, satisfies

$$(H-E)\,\Psi=0\,. \tag{2·3}$$

In order to expand Ψ in terms of the p-n relative wave functions, we introduce $\{\phi_0(\boldsymbol{\rho}),\,\phi_{lm}(k,\boldsymbol{\rho})\}$ as a complete set of orthonormalized eigenfunctions of p-n Hamiltonian, H_{pn}, where $\phi_0(\boldsymbol{\rho})$ is the deuteron internal s-wave function and $\phi_{lm}(k,\boldsymbol{\rho})$ the p-n continuum wave function having the momentum $\hbar k$, the angular momentum l and its z-component m. The eigenenergies of ϕ_0 and $\phi_{lm}(k)$ are $\varepsilon_0=-2.226$ MeV and $\varepsilon_k=\hbar^2k^2/2\mu_\rho$, respectively. $\phi_{lm}(k,\boldsymbol{\rho})$ is normalized as $\langle\phi_{lm}(k)|\phi_{lm}(k')\rangle=\delta(k-k')$ and its asymptotic form is given by

$$\phi_{lm}(k,\boldsymbol{\rho})\longrightarrow\sqrt{\frac{2}{\pi}}\sin\left(k\rho-\frac{l\pi}{2}+\delta_l\right)\cdot\rho^{-1}i^l\,Y_{lm}(\hat{\boldsymbol{\rho}}). \tag{2·4}$$

The asymptotic form includes the incoming wave, but its amplitude vanishes through the k-integration in the total three-body wave function.[3)]

As mentioned in § 1, we truncate l and k by

$$l\le l_{\max}\,,\qquad k\le k_{\max}\,. \tag{2·5}$$

The total wave function Ψ is then approximated by

$$\Psi=\sum_{JM}C_{JM}\psi_{JM}(\boldsymbol{R},\boldsymbol{\rho})\,Y^*_{JM}(\hat{\boldsymbol{P}}_0), \tag{2·6}$$

$$\psi_{JM}(\boldsymbol{R},\boldsymbol{\rho})=\phi_0(\boldsymbol{\rho})\chi_{JM}(P_0,\boldsymbol{R})+\sum_{l=0}^{l_{\max}}\sum_{|J-l|\le L\le J+l}\int_0^{k_{\max}}[\phi_l(k,\boldsymbol{\rho})\otimes\chi^{(J)}_{lL}(P,\boldsymbol{R})]_{JM}dk\,. \tag{2·7}$$

The constant C_{JM} depends on the normalization of the incident channel wave function. Here, J is the total angular momentum and L the angular momentum of the p-n c.m. motion. The wave functions, $\chi_{JM}(P_0,\boldsymbol{R})$ and $\chi^{(J)}_{lLM_L}(P,\boldsymbol{R})$, describe the p-n c.m. motion with the momentum $\hbar P_0$ in the elastic channel and that with $\hbar P$ in breakup channels, respectively; these momenta are determined by the conservation of the total energy.

The coupled-continuum-channels equations for χ's are given by**)

$$\langle[\phi_0\otimes i^J\,Y_J(\hat{\boldsymbol{R}})]_{JM}|H-E|\psi_{JM}\rangle_{\rho,\hat{R}}=0\,, \tag{2·8a}$$

$$\langle[\phi_l(k)\otimes i^L\,Y_L(\hat{\boldsymbol{R}})]_{JM}|H-E|\psi_{JM}\rangle_{\rho,\hat{R}}=0\,.\quad(k\le k_{\max},\ l\le l_{\max}) \tag{2·8b}$$

*) Due to this approximation, the Coulomb breakup (distortion) effect is neglected, but the distortion effect was found[17)] to be rather small even in the case $E_d=22$ MeV of $d+{}^{58}$Ni scattering.

**) $\langle\ \rangle_{\rho,\hat{R}}$ denotes the integration over $\boldsymbol{\rho}$ and $\hat{\boldsymbol{R}}$.

The asymptotic behaviour of χ's are given by

$$\chi_{JM}(P_0, \boldsymbol{R}) \longrightarrow [U_J^{(-)}(P_0, R) - S_J U_J^{(+)}(P_0, R)] \cdot R^{-1} i^J Y_{JM}(\hat{\boldsymbol{R}}), \tag{2·9a}$$

$$\chi^{(J)}_{lLM_L}(P, \boldsymbol{R}) \longrightarrow -\sqrt{\frac{P_0}{P}} S^{(J)}_{lL(k)} U_L^{(+)}(P, R) \cdot R^{-1} i^L Y_{LM_L}(\hat{\boldsymbol{R}}) \tag{2·9b}$$

for the open channels ($E - \varepsilon_k > 0$), while by the exponentially damping behaviour for the closed channels. The functions $U^{(\pm)}$ are defined by $U_L^{(\pm)}(P, R) = G_L(P, R) \pm iF_L(P, R)$, where $F_L(G_L)$ is the regular (irregular) Coulomb function.

2.2. *Coupled-discretized-continuum-channels (CDCC) method*

In this subsection we reformulate the CDCC method of Ref. 2); this method is different from that of Ref. 3), but the difference is negligible when Δk is sufficiently small. The truncated momentum space $k=0$ through $k_{\max}$ is discretized into momentum bins $\{[k_{i-1}, k_i],\ i=1 \sim N_b\}$ with $k_0 = 0$ and $k_{N_b} = k_{\max}$. The number of bins, N_b, and the intervals Δk_i ($= k_i - k_{i-1}$) can generally depend on the p-n relative angular momentum l, but we drop the index l from them for simplicity. The k-integration in Eq. (2·7) is then rewritten as

$$\begin{aligned} B &\equiv \int_0^{k_{\max}} [\phi_l(k, \boldsymbol{\rho}) \otimes \chi^{(J)}_{lL}(P, \boldsymbol{R})]_{JM} dk \\ &= \sum_{i=1}^{N_b} \int_{k_{i-1}}^{k_i} [\phi_l(k, \boldsymbol{\rho}) \otimes \chi^{(J)}_{lL}(P, \boldsymbol{R})]_{JM} dk\,. \end{aligned} \tag{2·10}$$

Here, we take the following two assumptions. Firstly, we assume that $\chi^{(J)}_{lLM_L}(P, \boldsymbol{R})$ depends little on P in each bin; we approximate B as

$$B \simeq \sum_{i=1}^{N_b} [\hat{\phi}_{il}(\boldsymbol{\rho}) \otimes \hat{\chi}^{(J)}_{ilL}(\boldsymbol{R})]_{JM} \tag{2·11}$$

with the definition

$$\hat{\phi}_{ilm}(\boldsymbol{\rho}) = \frac{1}{\sqrt{\Delta k_i}} \int_{k_{i-1}}^{k_i} \phi_{lm}(k, \boldsymbol{\rho}) dk\,, \tag{2·12}$$

$$\hat{\chi}^{(J)}_{ilLM_L}(\boldsymbol{R}) = \sqrt{\Delta k_i}\, \chi^{(J)}_{lLM_L}(P_i, \boldsymbol{R}). \tag{2·13}$$

From the orthonormal property of $\phi_0(\boldsymbol{\rho})$ and $\phi_{lm}(k, \boldsymbol{\rho})$, we obtain

$$\langle \hat{\phi}_{ilm} | \hat{\phi}_{i'l'm'} \rangle = \delta_{ii'} \delta_{ll'} \delta_{mm'}\,, \tag{2·14}$$

$$\langle \hat{\phi}_{ilm} | H_{pn} | \hat{\phi}_{i'l'm'} \rangle = \hat{\varepsilon}_i \delta_{ii'} \delta_{ll'} \delta_{mm'} \tag{2·15}$$

with

$$\hat{\varepsilon}_i = \frac{\hbar^2}{2\mu_\rho} \hat{k}_i^{\,2}\,, \tag{2·16}$$

$$\hat{k}_i^{\,2} = \left(\frac{k_i + k_{i-1}}{2}\right)^2 + \frac{1}{12}(\Delta k_i)^2\,, \tag{2·17}$$

where we have introduced the notations of $\hat{\phi}_{000}(\boldsymbol{\rho})=\phi_0(\boldsymbol{\rho})$ and $\hat{\varepsilon}_0=\varepsilon_0$ for the deuteron (ground) state. The p-n c.m. momentum P_i for the i-th bin is determined by

$$E=\varepsilon_0+\frac{\hbar^2}{2\mu_R}P_0^2=\hat{\varepsilon}_i+\frac{\hbar^2}{2\mu_R}P_i^2\,. \tag{2·18}$$

Secondly, we take the assumption that the *continuum* of Eq. (2·8b) in the momentum range $k_{i-1}\leq k\leq k_i$ can be replaced by *one* equation of

$$\langle[\hat{\phi}_{il}\otimes i^L Y_L(\hat{\boldsymbol{R}})]_{JM}|H-E|\psi_{JM}\rangle_{\rho,\hat{R}}=0\,. \tag{2·19}$$

Here, we introduce the radial wave functions $\hat{\chi}^{(J)}_{il}(R)$ by

$$\hat{\chi}_{JM}(P_0,\boldsymbol{R})=\hat{\chi}^{(J)}_{00J}(R)\cdot R^{-1}i^J Y_{JM}(\hat{\boldsymbol{R}}), \tag{2·20a}$$

$$\hat{\chi}^{(J)}_{ilLM_L}(\boldsymbol{R})=\hat{\chi}^{(J)}_{il}(R)\cdot R^{-1}i^L Y_{LM_L}(\hat{\boldsymbol{R}}). \tag{2·20b}$$

We then obtain the CDCC equations for the $\hat{\chi}(R)$'s:

$$\left[-\frac{\hbar^2}{2\mu_R}\frac{d^2}{dR^2}+\frac{\hbar^2}{2\mu_R}\frac{L(L+1)}{R^2}+U^{(\mathrm{Coul})}(R)-(E-\hat{\varepsilon}_i)\right]\hat{\chi}^{(J)}_{il}(R)$$
$$=-\sum_{i'=0}^{N_b}\sum_{l'=0}^{l_{\max}}\sum_{|J-l'|\leq L\leq J+l'}F^{(J)}_{il,i'l'L}(R)\hat{\chi}^{(J)}_{i'l'}(R) \tag{2·21}$$
$$(i=0\sim N_b,\ l=0\sim l_{\max},\ |J-l|\leq L\leq J+l)$$

with the form factors defined by

$$F_{il\,L,i'l'L'}(R)=\langle[\hat{\phi}_{il}\otimes i^L Y_L(\hat{\boldsymbol{R}})]_{JM}|U_{nA}+U_{pA}|[\hat{\phi}_{i'l'}\otimes i^{L'}Y_{L'}(\hat{\boldsymbol{R}})]_{JM}\rangle_{\rho,\hat{R}}\,. \tag{2·22}$$

The boundary condition for $\hat{\chi}^{(J)}_{il}$'s ($i=0\sim N_b$) in the asymptotic region is given by

$$\hat{\chi}^{(J)}_{il}(R)\longrightarrow U^{(-)}_l(P_0,R)\delta_{i0}\delta_{l0}\delta_{LJ}-\sqrt{\frac{P_0}{P_i}}\hat{S}^{(J)}_{il\,L}U^{(+)}_L(P_i,R) \tag{2·23}$$

for the open channels ($E-\hat{\varepsilon}_i>0$) and by the asymptotically vanishing condition for the closed channels.

Finally, from the before-mentioned assumption that $\chi^{(J)}_{lL}(P,R)$ depends little on P in each bin, the breakup S-matrix elements $S^{(J)}_{lL}(k)$ in Eq. (2·9b) for the p-n *continuum* are approximated by

$$S^{(J)}_{lL}(k)\simeq\hat{S}^{(J)}_{il\,L}/\sqrt{\Delta k_i}\,,\qquad k_{i-1}\leq k\leq k_i\,,\quad (i=1\sim N_b) \tag{2·24a}$$

while the elastic S-matrix element in Eq. (2·9a) is approximated by

$$S_J \simeq \widehat{S}^{(U)}_{00J} . \qquad (2\cdot24b)$$

A better approximation than Eq. (2·24a) can be obtained by seeking a smooth function that has the value $S^{(U)}_{\ell\ell}(\widehat{k}_i)$ at every position of $k=\widehat{k}_i$.

In the following calculations, we take the equal-width momentum bins; namely, $\Delta k_i=\Delta k$ ($i=1\sim N_b$). It is naturally expected that, as the width Δk becomes small, the S-matrix elements (2·24) calculated by the CDCC method converge to ones by the coupled-continuum-channels method (2·8), though its mathematical proof has not yet been reported so far.

2.3. *Potentials adopted*

Throughout the following calculations, ^{58}Ni nucleus is taken to be the target, and $E_d=80$ MeV in laboratory system. The nucleon-target potentials, $U_{pA}(r_{pA})$ and $U_{nA}(r_{nA})$, are phenomenological potentials of Becchetti and Greenlees,[18),*)] corresponding to one half of the deuteron incident energy. The proton-neutron potential $V_{pn}(\rho)$ is $-v_0\exp[-(\rho/\rho_0)^2]$ with $v_0=72.15$ MeV and $\rho_0=1.484$ fm for any p-n partial wave l;[19)] this V_{pn} well reproduces low-energy p-n scattering data (we have examined that the following discussion is little affected by the choice of V_{pn}, even in the case of a soft core potential included).

The form factors (2·22) are calculated by a direct numerical method up to $R=20$ fm. The integration over ρ in Eq. (2·22) is made up to $\rho=40$ fm and the integration over k in Eq. (2·12) is performed numerically with the k-interval of 0.01 fm^{-1}; these give accurate form factors of (2·22) in the region $R\leq 20$ fm. The familiar type of coupled-channels equations (2·21) is solved by the direct numerical method;[20)] the matching radius is taken to be $R=20$ fm.

§ 3. Validity of the CDCC method; convergence with narrowing Δk

In this section, we shall examine the validity of the CDCC method by checking the convergence of the elastic and the breakup S-matrix elements (cross sections) with respect to narrowing Δk in the cases of the adiabatic Hamiltonian and the exact one (though the Coulomb potential is not of the three-body type).

In the cases of the both Hamiltonians, we fix the upper limit of the p-n relative momentum to $k_{\max}=1.5$ fm^{-1} ($\widehat{\varepsilon}_{N_b}=93.4$ MeV) and take the p-n relative angular momentum to be $l=0$ and 2 in solving the CDCC equations; the effect of p-wave ($l=1$) and g-wave ($l=4$) is found to be negligible.

*) The optical potential parameters are given, in the usual notation, by $V_0=44.921$ MeV, $a_V=0.75$ fm, $r_V=1.17$ fm, $W_0=6.100$ MeV, $a_W=a_{WD}=0.534$ fm, $r_W=r_{WD}=1.32$ fm, $W_D=2.214$ MeV for proton and by $V_0=42.672$ MeV, $a_V=0.75$ fm, $r_V=1.17$ fm, $W_0=7.240$ MeV, $a_W=a_{WD}=0.580$ fm, $r_W=r_{WD}=1.26$ fm, $W_D=2.586$ MeV for neutron. The Coulomb radius of $U^{(Coul)}$ is taken to be $R_C=4.919$ fm.

3.1. *Test on the adiabatic Hamiltonian*

The adiabatic Hamiltonian, $H_{\rm AD}$, is introduced[1),6)] by

$$H_{\rm AD}=-\frac{\hbar^2}{2\mu_R}\nabla_R^2+U_{nA}(r_{nA})+U_{pA}(r_{pA})+U^{(\rm Coul)}(R)+\varepsilon_0\,. \tag{3·1}$$

Here, H_{pn} of Eq. (2·1) is replaced by the deuteron internal energy ε_0. The three-body wave function in the adiabatic approximation, $\Psi_{\rm AD}$, satisfies

$$(H_{\rm AD}-E)\,\Psi_{\rm AD}=0\,. \tag{3·2}$$

This equation is solved by two methods. One is the direct numerical method[6)] which gives the exact solution. The other is the CDCC method. In the framework of the latter method, we set $\tilde{\varepsilon}_i=\tilde{\varepsilon}_0$ $(=\varepsilon_0)$ $(i=1\sim N_b)$ in Eq. (2·21) for all the partial waves of the p-n relative motion. Results are shown in Figs. 1~3 for the cases $\Delta k=1/2$, 1/4, 1/6 and 1/8 fm^{-1}.

In Fig. 1, squared moduli of the deuteron s-wave breakup S-matrix elements $S^{(J)}_{l=0,L=J}(k)$ and the d-wave ones $S^{(J)}_{l=2,L=J-2}(k)$, $S^{(J)}_{l=2,L=J}(k)$, $S^{(J)}_{l=2,L=J+2}(k)$ are plotted for the case $J=17$ at which the largest partial breakup cross section is obtained (cf. Fig. 2).They smoothly converge to the exact ones. It is confirmed that real phase shifts of the above S-matrix elements also converge as observed in Fig. 1(a) of Ref. 8b) for the deuteron s-wave breakup in $d+^4$He scattering.

The k-integrated partial breakup cross section is introduced by

$$\sigma^{(J)}_l=\frac{\pi(2J+1)}{P_0^2}\sum_{|J-l|\le L\le J+l}\int_0^{k_{\rm open}}|S^{(J)}_{lL}(k)|^2\,dk\,. \tag{3·3}$$

The upper limit of the integration, $k_{\rm open}$, is given by $E-\hbar^2k^2_{\rm open}/2\mu_\rho=0$. In Fig. 2, fast convergence is shown for $\sigma^{(J)}_l$ $(l=0, 2)$. The case $\Delta k=1/2$ fm^{-1} agrees fairly well with the exact solution in the region around the peak, and the case $\Delta k=1/6$ fm^{-1} is in excellent agreement with the exact one. It is to be noted that the convergence is much faster than seen in Fig. 1 for $|S^{(J)}_{lL}(k)|^2$ on account of the k-integration.

In Fig. 3, we also recognize fast convergence for the elastic scattering cross sections; even in the case $\Delta k=1/4$ fm^{-1} the cross section agrees with the exact one. In fact, the convergence of the elastic scattering cross section is even faster than the k-integrated partial breakup cross sections. This is reasonable because the elastic scattering cross section contains the breakup effects only in second order.

From the above analysis, it is concluded that the solution of the CDCC equation converges toward the exact one.

3.2. *Test on the exact Hamiltonian*

The width of the momentum bins is changed as $\Delta k=1/4$, 1/6, 1/8 and 1/10

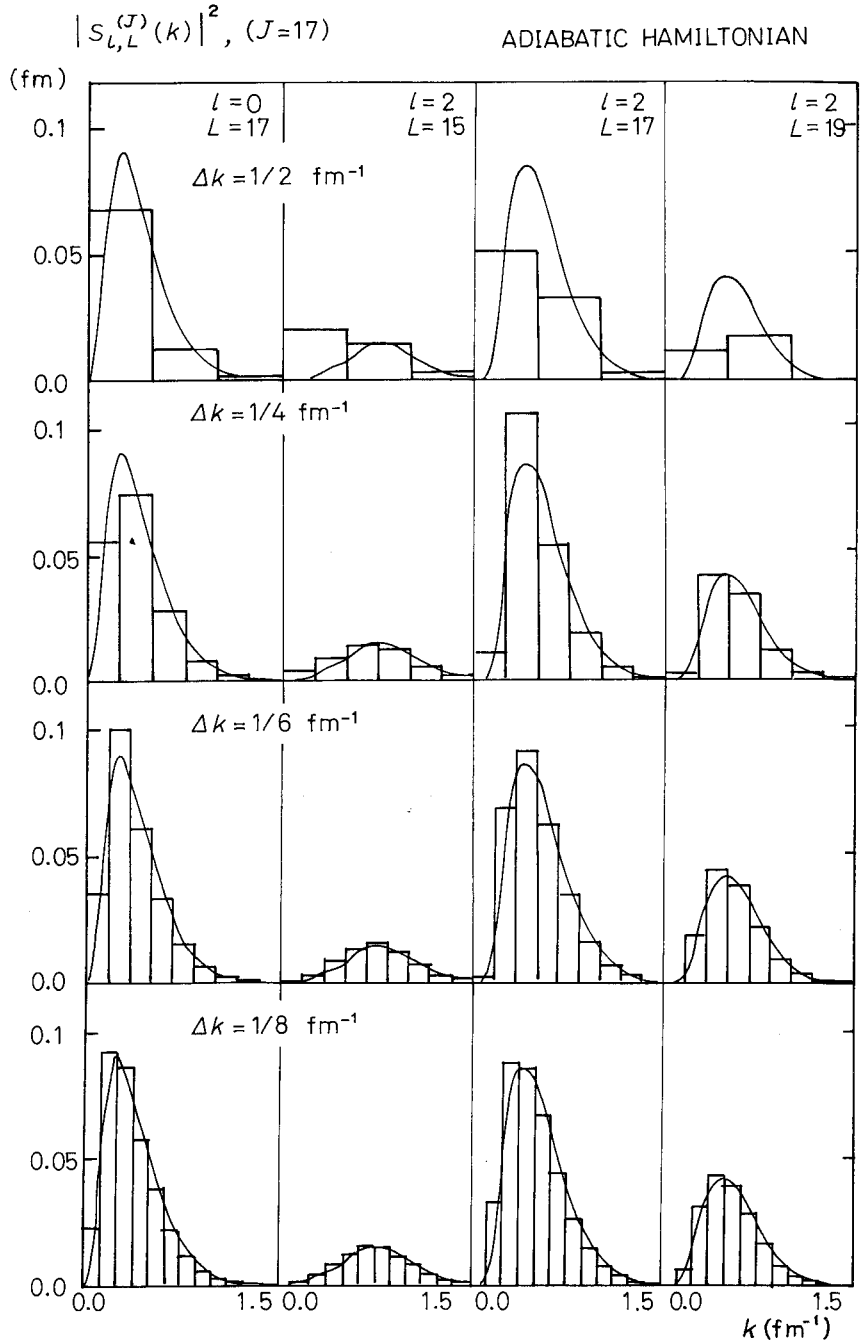

Fig. 1. Convergence of squared moduli of the breakup S-matrix element $S_{l,L}^{(J)}(k)$ with respect to narrowing Δk for the case of the *adiabatic* Hamiltonian ($J=17$). The step lines are given by the CDCC method, while the smooth solid lines stand for the exact solution. The leftmost is for the s-wave ($l=0$) breakup and the other three for the d-wave ($l=2$) breakup ($L=J-2$, J and $J+2$).

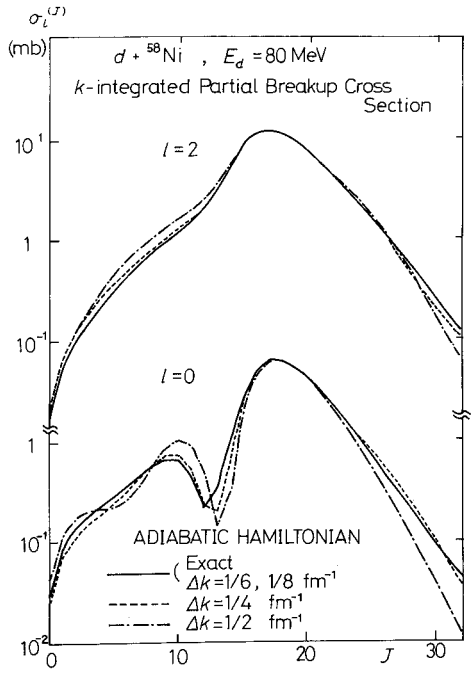

Fig. 2. Convergence of the partial breakup cross sections $\sigma_l^{(J)}$ (for $l=0$ and 2 at $J=17$) with respect to narrowing Δk for the case of the *adiabatic* Hamiltonian.

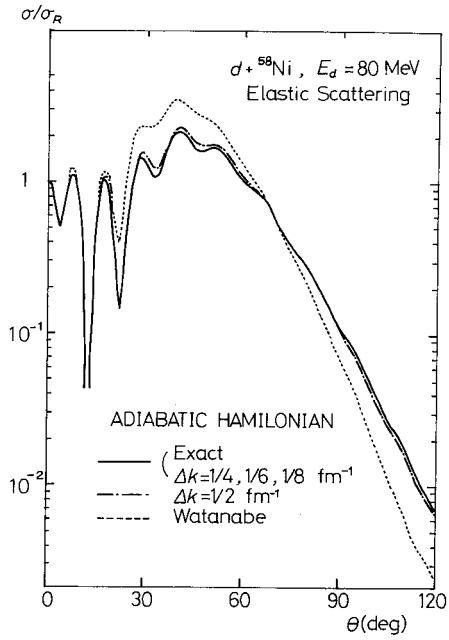

Fig. 3. Convergence of the elastic scattering cross section of $d+{}^{58}Ni$ with Δ_k narrowing for the case of the *adiabatic* Hamiltonian. The exactly calculated cross section is also shown. Result by Watanabe model [22] (namely the case $N_b=0$) is also illustrated. The cross sections are given in ratio to the Rutherford cross section.

fm^{-1} in this subsection.

In Fig. 4, the histogram shows the s-wave and the d-wave breakup S-matrix elements; the folded lines in the case $\Delta k=1/10$ fm^{-1} are drawn through $S_{l,l}^{(J)}(k)$'s at $k=\hat{k}_1, \cdots, \hat{k}_{N_b}$; the same lines are plotted again in the figures for the other cases of Δk to guide the eye in seeing the convergence. We clearly see that the S-matrix elements are smoothly converging as Δk narrows. In the light of the discussion in § 3.1, it may be said that the folded lines must be very close to the exact results (though we do not have them in hand for the case of the exact Hamiltonian). Also confirmed is the convergence of real phase shifts, though not illustrated. The convergence is also seen for any total angular momentum J.

As shown in Figs. 5 and 6, clear convergence is recognized both for the k-integrated partial breakup cross sections $\sigma_l^{(J)}$ and for the elastic scattering cross sections. The curves $\Delta k=1/6$ and 1/8 fm^{-1} overlap to each other in $\sigma_l^{(J)}$, while the curve $\Delta k=1/4$ fm^{-1} already agrees with those of $\Delta k=1/6$, 1/8 and 1/10 fm^{-1} for

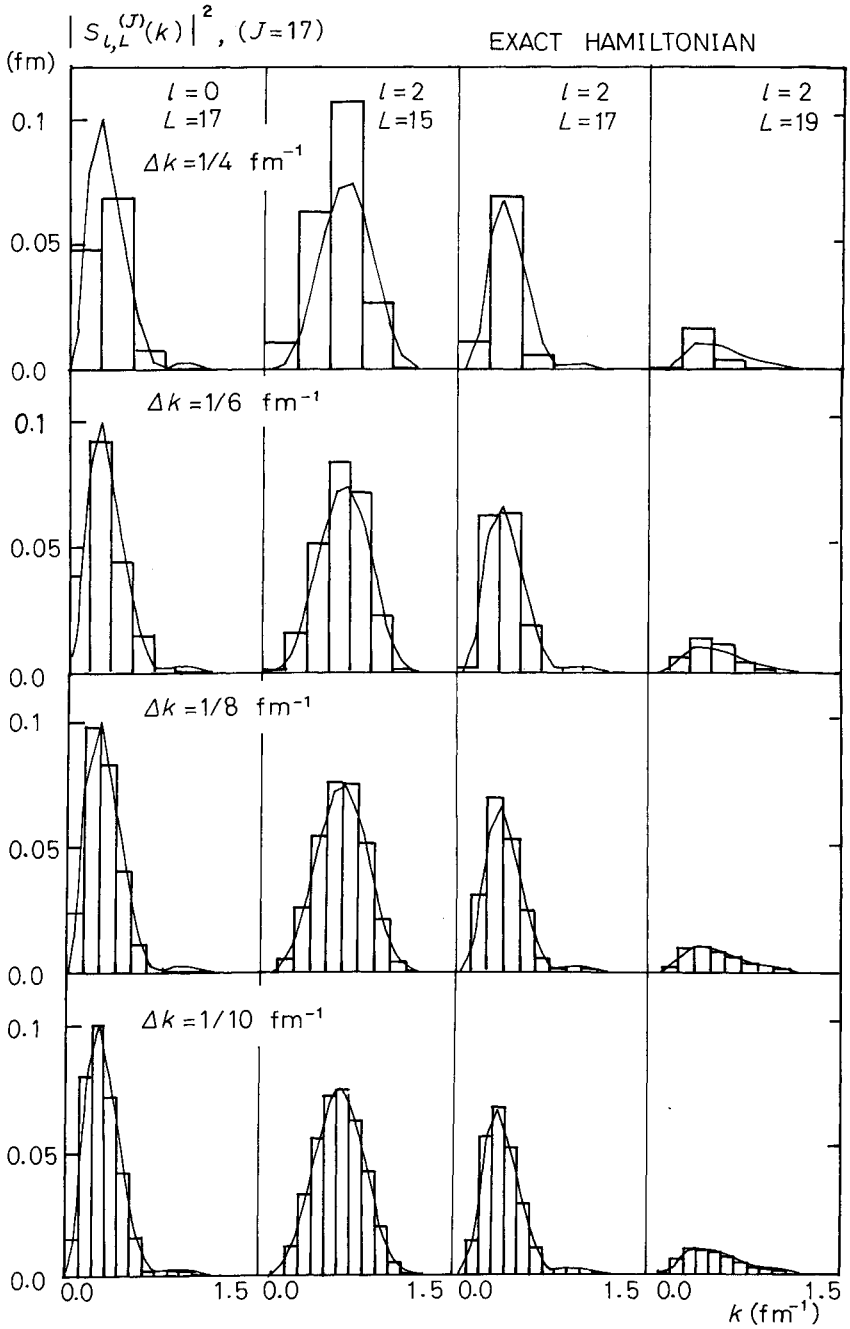

Fig. 4. Same as Fig. 1 for the case of the *exact* Hamiltonian. As for the thin folded solid lines, see the text.

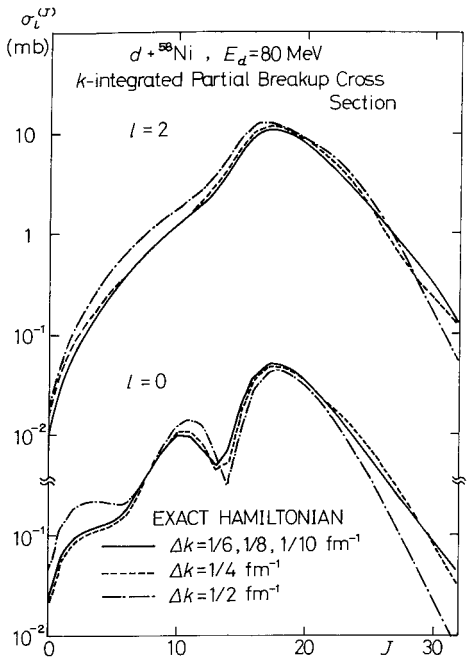

Fig. 5. Same as Fig. 2 for the case of the *exact* Hamiltonian.

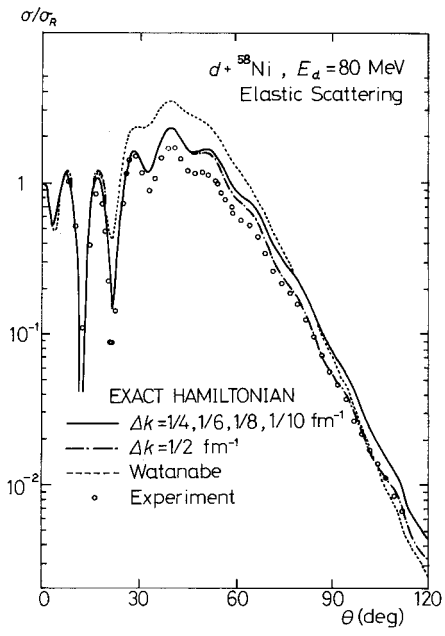

Fig. 6. Same as Fig. 3 for the case of the *exact* Hamiltonian. Experimental data[21] are also shown.

the elastic scattering cross section. One may consider that such converged curves stand for the exact results. It is thus found that the sufficient convergence is given by the calculation with $\Delta k = 1/4$ fm^{-1} for the elastic scattering cross section, with $\Delta k = 1/6$ fm^{-1} for the k-integrated partial breakup cross sections and with $\Delta k = 1/8$ fm^{-1} for the breakup S-matrix elements; this is the same as the case of the adiabatic Hamiltonian.

The converged elastic scattering cross section is in good agreement with the experimental data for the scattering angle $\theta \lesssim 30^\circ$, but not for $\theta \gtrsim 30^\circ$. Further discussions on the cross section as well as that of the $E_d = 22$ MeV case will be made in a forthcoming paper on the basis of the detailed analysis of the multi-step breakup processes.

§ 4. Truncation of $k_{\max}$ and $l_{\max}$

In this section, solving Eq. (2·21) for the exact Hamiltonian, we shall analyze the convergence of the elastic and the breakup partial cross sections with respect to increasing $k_{\max}$ and $l_{\max}$ in order to investigate $k_{\max}$ and $l_{\max}$ which give a physically sufficient truncation of the model space.

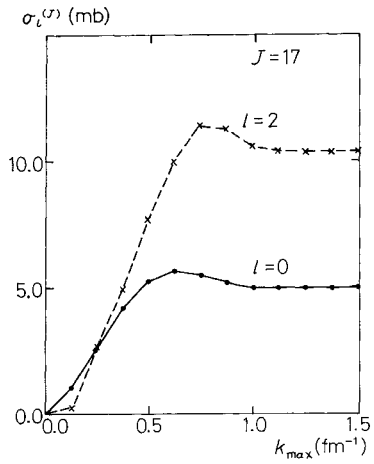

Fig. 7. Convergence of the k-integrated partial ($J=17$) breakup cross sections ($l=0$ and 2) with respect to increasing k_{max}.

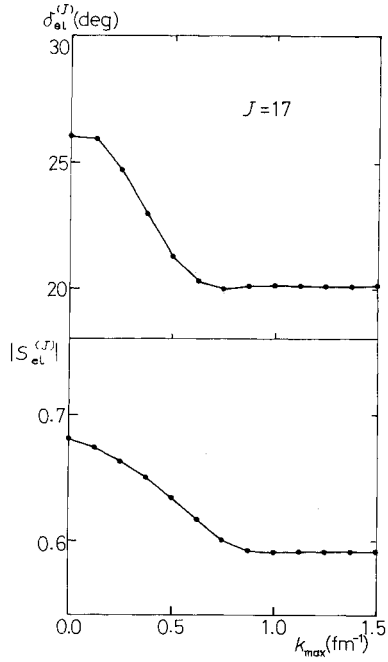

Fig. 8. Convergence of the elastic S-matrix element ($J=10$) with respect to increasing k_{max}.

4.1. *Convergence with increasing* k_{max}

Taking the case in which the width of momentum bins is fixed at $\Delta k=1/8$ fm^{-1} and the s- and d-waves of the p-n systems are coupled to each other, we examine the convergence of the solution given by the CDCC method with respect to increasing k_{max} up to 1.5 fm^{-1}. Figure 7 shows the k-integrated partial breakup cross sections for the s- and d-waves at $J=17$. Clear convergence around $k_{max}=9/8$ fm^{-1} is obtained.

In Fig. 8, another convergence is observed around $k_{max}=7/8$ fm^{-1} for the modulus and the phase of the elastic S-matrix element at $J=17$. Again we recognize that the convergence seen in the elastic scattering is faster than in the breakup reactions. It has been confirmed that $k_{max}=1.0$ fm^{-1} is sufficient for all J's as far as the elastic scattering and the k-integrated partial breakup cross sections are concerned. The continuum states in $1.0\text{ fm}^{-1}<k<1.5\text{ fm}^{-1}$ give little effect on the k-dependence of the breakup S-matrix elements in Fig. 4.

4.2. *Convergence with increasing* l_{max}

In this subsection, we examine the effects of the p-n relative waves other than

Table I. Role of the truncation of the p-n relative angular momentum in partial breakup, elastic and reaction cross sections for $J=17$.

partial cross sections ($J=17$) (mb)	s	$s+d$	$s+d+g$	$s+d+g+i$	$s+d+g+i+p$
$\sigma_s^{(J)}$	10.725	4.067	3.930	3.989	3.988
$\sigma_d^{(J)}$		12.596	11.651	11.351	11.356
$\sigma_g^{(J)}$			1.830	1.684	1.688
$\sigma_i^{(J)}$				0.202	0.202
$\sigma_p^{(J)}$					0.033
$\sum_l \sigma_l^{(J)}$	10.725	16.663	17.411	17.226	17.267
$\sigma_{\mathrm{el}}^{(J)}$	90.106	74.230	73.502	73.658	73.634
$\sigma_{\mathrm{reac}}^{(J)}$	93.429	99.444	100.32	100.33	100.35

the s- and d-waves by making CDCC calculations with the s-, d-, g-, i- and p-waves included. The effects of the odd waves are small, because the couplings between the even and the odd waves come from the small difference of the p- and n-target optical potentials, i.e., $U_{pA}(r_{pA})-U_{nA}(r_{pA})$. In order to see the significance of the p-n partial waves mentioned above, we take the case $\Delta k=1/2$ fm^{-1} and $k_{\max}=1.0$ fm^{-1}; this truncation may be sufficient for this limited purpose.

Table I lists the k-integrated partial breakup cross sections to the s-, d-, g-, i- and p-waves, $\sigma_s^{(J)}$, $\cdots$, $\sigma_p^{(J)}$, and the partial elastic cross section defined by $\sigma_{\mathrm{el}}^{(J)}=\pi(2J+1)/P_0^2|1-S_{\mathrm{el}}^{(J)}|^2$, $S_{\mathrm{el}}^{(J)}$ being the *nuclear* elastic S-matrix element; again we take the case $J=17$. The columns 2 through 6 stand for the types of CDCC calculations which include the s-wave breakup, the s- and d-wave breakup and so forth. We can see the sufficient convergence with increasing $l_{\max}$ and the dominant role of the s- and d-waves. Though the g-wave breakup cross sections $\sigma_g^{(J=17)}$ amount to about 10% of the l-summed breakup cross sections at $J=17$, the coupling of the g-wave breakup states to the s- and d-wave ones is found to be rather small; this weakness of the coupling is more evident for the i- and p-waves. The f-wave is more negligible than the p-wave. The couplings of the g-, i- and p-wave breakup channels to the elastic channel are also found to be negligible. We can expect that it is a good approximation to calculate the breakup cross sections for the p-n partial waves other than the s- and d-waves by means of the CCBA treatment based on the CDCC wave functions of the incident channel and the s- and d-wave breakup channels.

§ 5. Conclusions

We have verified the validity of the CDCC (coupled-discretized-continuum-channels) method for the treatment of the deuteron breakup process by examining

the convergence of the elastic and the breakup S-matrix elements (cross sections) with respect to narrowing width of the discretized p-n momentum bins, Δk. In the case of the adiabatic three-body Hamiltonian (3·1), we have observed the solution obtained by the CDCC method really converges to the exact one. In the case of the exact three-body Hamiltonian (2·1), the S-matrix elements converge smoothly as Δk narrows. The converged S-matrix elements can be regarded as the S-matrix elements of the coupled-continuum-channels equation (2·8) on the basis of the result in the case of the adiabatic Hamiltonian.

For the $d+^{58}$Ni system at $E_d=80$ MeV, it has been found that the sufficient convergence is obtained with $\Delta k=1/4\,\mathrm{fm}^{-1}$ for the elastic scattering cross section, with $\Delta k=1/6\,\mathrm{fm}^{-1}$ for the k-integrated partial breakup cross sections and with $\Delta k=1/8\,\mathrm{fm}^{-1}$ for the breakup S-matrix elements. This is the same as in the case of the adiabatic Hamiltonian.

It has been shown that the elastic and the k-integrated partial breakup cross sections converge with increasing $k_{\max}$ and $l_{\max}$. The physically sufficient truncation is given by $l=0$ and 2 and $k_{\max}\sim 1.0\,\mathrm{fm}^{-1}$ for the elastic and the k-integrated partial breakup cross sections. The g-wave breakup amounts to abount 10% of the l-summed breakup cross section at $J=17$, and the i- and p-wave breakup are negligible. The coupling of the g-, i- and p-waves to the elastic channel is very small. For detailed discussions of the breakup S-matrix elements $S^{(J)}_{l,L}(k)$ it is recommended to take $\Delta k=1/8\,\mathrm{fm}^{-1}$, $k_{\max}=1.5\,\mathrm{fm}^{-1}$ and $l=0$ and 2.

Also in the case $E_d=22$ MeV, sufficient convergence is confirmed with the case of the same Δk and $k_{\max}$ as in the case $E_d=80$ MeV. The g-wave breakup cross section, however, becomes twice as much as that of the 80 MeV case mentioned above.[16]

The present work gives a good basis for the CDCC method for deuteron induced reactions. The method is useful for studies not only of the deuteron breakup effect on the elastic scattering but also of the breakup process itself on account of the correct asymptotic behaviour of p-n continuum states. This method is found to be also useful for the study[23] of heavy-projectile (such as ^{6}Li, ^{7}Li and ^{9}Be) induced reactions in which the breakup process is suggested to be important.[24]

Acknowledgements

The authors would like to thank Professor M. Kawai for stimulating discussion. The numerical calculation was done at the Computer Center of Kyushu University with financial support from the Research Center for Nuclear Physics, Osaka University. One of the authors (M.N.) would like to thank Professor T. Maki for his continuous encouragement.

References

1) R. C. Johnson and P. J. R. Soper, Phys. Rev. **C1** (1970), 976.
J. D. Harvey and R. C. Johnson, Phys. Rev. **C3** (1971), 636.
2) G. H. Rawitscher, Phys. Rev. **C9** (1974), 2210.
3) J. P. Farrell, Jr., C. M. Vincent and N. Austern, Ann. of Phys. **96** (1976), 333.
N. Austern, C. M. Vincent and J. P. Farrell, Jr., Ann. of Phys. **114** (1978), 93.
4) B. Anders and A. Lindner, Nucl. Phys. **A296** (1978), 77.
5) M. Kawai, M. Kamimura and K. Takesako, *Proceedings of 1978 INS International Symposium on Nuclear Direct Reaction Mechanism, Fukuoka, 1978,* pp. 710, 711, 712.
M. Kawai, ibid, p. 464.
6) H. Amakawa, S. Yamaji, A. Mori and K. Yazaki, Phys. Letters **82B** (1979), 13.
H. Amakawa and K. Yazaki, Phys. Letters **87B** (1979), 159.
7) H. Nishioka, S. Saito, H. Kanada and T. Kaneko, Prog. Theor. Phys. **63** (1980), 438.
H. Kanada, T. Kaneko, H. Nishioka and S. Saito, Prog. Theor. Phys. **63** (1980), 842.
8a) M. Yahiro and M. Kamimura, Prog. Theor. Phys. **65** (1981), 2046.
b) M. Yahiro and M. Kamimura, Prog. Theor. Phys. **65** (1981), 2051.
9) A. W. Thomas, *Lecture Notes in Physics,* edited by H. Zingl, M. Haftel and H. Zankel, vol. 87 (Springer-Verlag 1978), p. 247.
10) P. E. Shanley, Phys. Rev. **187** (1969), 1328.
B. Charnomordic, C. Fayard and G. H. Lamot, Phys. Rev. **C15** (1977), 864.
Y. Koike, Nucl. Phys. **A337** (1980), 23.
11) L. D. Faddeev, Soviet Phys.-JETP **12** (1961), 1041.
12) C. Stolk and J. A. Tjon, Phys. Rev. Letters **35** (1975), 985.
J. J. Benayoun, J. Chauvin, C. Gignoux and A. Laverne, Phys. Rev. Letters **36** (1976), 1438.
13) T. Sasakawa, H. Okuno, T. Sawada, Phys. Rev. **23** (1981), 905.
14) R. G. Newton, *Scattering Theory of Waves and Particles* (McGraw-Hill Book Co., NewYork, 1966), chap. 17.
15) K. Takeuchi, Nucl. Phys. **A208** (1973), 1, 21, 46.
16) Y. Iseri, M. Nakano, M. Yahiro and M. Kamimura, private communications.
17) W.-M. Wendler, A. Lindner and B. Anders, Nucl. Phys. **A349** (1980), 365.
18) F. D. Becchetti, Jr. and G. W. Greenlees, Phys. Rev. **182** (1969), 1190.
19) T. Ohmura, B. Imanishi, M. Ichimura and M. Kawai, Prog. Theor. Phys. **43** (1970), 347.
20) T. Tamura, ORNL-4152, (1967).
P. Henrici, *Discrete Variable Methods in Ordinary Differential Equations* (John Wiley and Sons, New York, 1962).
21) E. J. Stephenson et al., *Proceedings of Fifth International Symposium on Polarization Phenomena in Nuclear Physics, Santa Fe,* ed. by G. G. Ohlsen et al., (American Institute of Physics, 1980), p. 484.
22) S. Watanabe, Nucl. Phys. 8 (1958), 484.
23) Y. Sakuragi, M. Yahiro and M. Kamimura, Prog. Theor. Phys. **68** (1982), No. 1.
24) G. R. Satchler and W. G. Love, Phys. Reports **55** (1979), 183.